دار المنظومة
DAR ALMANDUMAH
الرواد في قواعد المعلومات العربية

العنوان:	The Investigation of the effect of Various Parameters of Double Containment Joint of a Composite Structure
المؤلف الرئيسي:	Krayyem, Ahmad Mohammed
مؤلفين آخرين:	Sadek, Medhat M.(Super)
التاريخ الميلادي:	1990
موقع:	الكويت
الصفحات:	1 - 466
رقم MD:	586776
نوع المحتوى:	رسائل جامعية
اللغة:	English
الدرجة العلمية:	رسالة ماجستير
الجامعة:	جامعة الكويت
الكلية:	كلية الهندسة
الدولة:	الكويت
قواعد المعلومات:	Dissertations
مواضيع:	الهندسة الميكانيكية، تكنولوجيا التثبيت
رابط:	https://search.mandumah.com/Record/586776

© 2020 دار المنظومة. جميع الحقوق محفوظة.
هذه المادة متاحة بناء على الإتفاق الموقع مع أصحاب حقوق النشر، علما أن جميع حقوق النشر محفوظة. يمكنك تحميل أو طباعة هذه المادة للاستخدام الشخصي فقط، ويمنع النسخ أو التحويل أو النشر عبر أي وسيلة (مثل مواقع الانترنت أو البريد الالكتروني) دون تصريح خطي من أصحاب حقوق النشر أو دار المنظومة.

المنارة للاستشارات
www.manaraa.com

ABSTRACT

Adhesive bonding added a new dimension to the technology of fastening. The bonding technique was applied successfully in different fields such as aircrafts, workshop machines, e.g.: fully bonded milling machine, and the gear box of a lathe machine, ... etc..

However, no attempts were made on optimizing the various parameters of the joint configuration on the basis of the strength of a double containment joint.

The work reported here is an investigation into the stress distributions in adhesive bonded double containment joint.

It is aimed at improving the joint performance under the static and dynamic loading and to give most possible uniform stress distribution along the adhesive layers, through the change of joint geometry.

A problem usually encountered with bonded joints is the differential straining of the adhesive and adherend materials which causes a state of highly localized stress discountinuity and so causes high stress concentration at the adhesive free edges.

It is shown that Poisson's ratio strains in the adherends of a double containment joint induce tranverse stresses both in the adhesive and in the adherends and so causing the differential straining.

The present investigation is aided by the finite element method using an established program called NASTRAN.

The two-dimensional finite element model (Plain Strain) was used to predict the normal and principal stresses of the bond layers in the static analysis and the natural frequencies of the system in the dynamic one.

The same different joint geometry parameters were investigated for both static and dynamic analyses.

Varying the cantilever depth inside the joint casing was taken as the first parameter of investigation. The results obtained indicated that by increasing the depth of the joint beam the strength increases up to certain limit. While it was found that there is no interpolation between the above parameter and the system natural frequency. The second parameter taken was the joint casing tapering, where it improved the joint strength but it reduced the system natural frequency.

It was found that by increasing the adhesive thickening at the free edge reduces the stress concentration and raises the joint natural frequency.

Real double containment joints, however, are formed with a fillet of adhesive spew, which was represented in the finite element models as a triangular fillet. The presence of the fillet significantly modifies the stress field in the highly-stressed regions at the ends of the overlap.

The significant stresses within the spew are shown to be tensile and at right angles to the direction of cracks. The maximum stress exists at the adherend corner within the fillet, but its value is dependent on the adherend corner shape.

The fillet existence is also recommended in the dynamic case where it raises the natural frequency of the system.

Finally since the adhesive bonding faciliates the joining of dissimilar materials, it is recommended generally to select the joint casing of lower Poisson's ratio than the cantilever.

From the present work an optimal joints were obtained for the static, dynamic and static/ dynamic applications, assuming linearly elastic behavior of the adhesive.

547224

الخلاصة

إن الربط باللاصق يعتبر إحدي عمليات التقنية الحديثة للتثبيت . وقد طبقت بنجاح في مجالات مختلفة منها الطائرات و مكائن الورش ، علي سبيل المثال لا الحصر ماكينة التفريز الملصقة بالكامل و صندوق المسننات لالة المخرطة ....الخ .

هذا ولم يتم أي محاولات لتحسين قوة الربطة مزدوجة الاحتواء علي أساس تغيير شكلها والتي هي موضوع البحث .

إن الهدف الرئيسي للبحث هو تطوير أداء الربطة مزدوجة الاحتواء وذلك لتحسين الصفات الاستاتية والدينامية لها أي للحصول علي توزيع منتظم للاجهاد وقيمة مرتفعة للذبذبة الطبيعية .

فمن المشاكل الرئيسية التي تواجه الربطات بالتلصيق هي الانفعالات التفاضلية بتأثير نسبة انفعلات بواصون والتي تسبب ارتفاع موضعي للاجهاد مسببة قيمة عالية جدا من الاجهاد المركز عند الوجه الحر للمادة اللاصقة .

في الموضوع الحالي تم استخدام طريقة العناصر المحددة الرياضية وذلك في برنامج ناستران (الصادر من وكالة الفضاء الامريكية ، ناسا) علي الحاسب الالي لجامعة الكويت . قد تم تمثيل الربطة علي أساس العناصر المحددة في البعدين والانفعالات السطحية وذلك للحصول علي الاجهادات الرئيسية في الطبقة اللاصقة والتذبذب الطبيعي للجسم .

بدراسة العديدمن العوامل وتأثيرها علي كفاءة الربطة مزدوجة الاحتواء تبين أن تغيير عمق القنطرة داخل الاحتواء حسّن من الصفات الاستاتية بزيادة العمق إلا أنه لم يكن له تأثير واضح علي التذبذب الطبيعي .

أما العامل الثاني فهو استدقاق طرف الاحتواء عند طرف الالصاق الحر والذي قلل من قيمة الاجهاد العالي في تلك المنطقة ولكنه أنقص من قيمة التذبذب الطبيعي .

كذلك وجد أنه بزيادة سماكة اللاصق عند الطرف الحر يقلل من قيمة تركيز الإجهاد وكذلك من قيمة التذبذب الطبيعي .

في الحقيقة عند تلصيق القنطرة بالاحتواء يخرج اللاصق الي الخارج مشكلا شرحة مثلثية عند الطرف مما يقلل كثيراً من قيمة الاجهاد المركز عند تلك المنطقة كما يقلل أيضاً من احتمال حدوث التمزق إضافة إلي تحسين الصفات الدينامية للجسم وذلك برفع قيمة الذبذبة الطبيعية .

من أهم مزايا تقنية اللصق هو تثبيت مادتين مختلفتين مع بعضهما الأمر الذي لا يمكن تحقيقه في اللحام التقليدي . وقد وجد من الدراسة الحالية إنه من الأفضل من الوجه الدينامية و الستاتية باستخدام مادة الاحتواء للربطة ذو قيمة بواصون النسبية أقل من تلك للقنطرة .

وبنهاية البحث أمكن استخلاص النتائج التالية : ربطة مزدوجة الاحتواء تُحسن من الخصائص الاستاتية وأخري من الخصائص الدينامية و الثالثة من الخصائص الاستاتية والدينامية معاً .

دار المنظومة
DAR ALMANDUMAH
الرواد في قواعد المعلومات العربية

العنوان:	The Investigation of the effect of Various Parameters of Double Containment Joint of a Composite Structure
المؤلف الرئيسي:	Krayyem, Ahmad Mohammed
مؤلفين آخرين:	Sadek, Medhat M.(Super)
التاريخ الميلادي:	1990
موقع:	الكويت
الصفحات:	1 - 466
رقم MD:	586776
نوع المحتوى:	رسائل جامعية
اللغة:	English
الدرجة العلمية:	رسالة ماجستير
الجامعة:	جامعة الكويت
الكلية:	كلية الهندسة
الدولة:	الكويت
قواعد المعلومات:	Dissertations
مواضيع:	الهندسة الميكانيكية، تكنولوجيا التثبيت
رابط:	https://search.mandumah.com/Record/586776

© 2020 دار المنظومة. جميع الحقوق محفوظة.
هذه المادة متاحة بناء على الإتفاق الموقع مع أصحاب حقوق النشر، علما أن جميع حقوق النشر محفوظة. يمكنك تحميل أو طباعة هذه المادة للاستخدام الشخصي فقط، ويمنع النسخ أو التحويل أو النشر عبر أي وسيلة (مثل مواقع الانترنت أو البريد الالكتروني) دون تصريح خطي من أصحاب حقوق النشر أو دار المنظومة.

المنارة للاستشارات
www.manaraa.com

Contents

		Page
Notation		i
List of tables		iv
List of figures		v
List of curves		vii
CHAPTER 1 :	Background and Introductory Material	1
1.1)	Historical review	1
1.2)	Object of the project	5
CHAPTER 2 :	Basis of Finite Element Method	11
2.1)	Introduction	11
2.2)	History	13
2.3)	Basic fundamentals	14
	2.3.1) Typical finite element analysis	14
	2.3.2) Assymbly or system analysis	17
2.4)	"Pseudo" Example of finite elements	19
2.5)	Coordinate systems	21
	2.5.1) Local coordinate systems	21
	2.5.2) Natural coordinate systems	21
	2.5.3) Global coordinate systems	21
	2.5.4) Rectangular element	21
	2.5.5) Triangular element : Area coordinates	22
2.6)	Theory of elasticity	22
	2.6.1) Stress, strain and Hooke's law	23
	2.6.2) The strain-displacements equations	24
	2.6.3) The element matrices	24
	2.6.4) Plane stress and plane strain	24
	2.6.4.1) Plane stress	24
	2.6.4.2) Plane strain	25
2.7)	Element analysis	26
	2.7.1) Shape functions	27
	2.7.2) Rectangular element	27
	2.7.2.1) First order rectangular element	27
	2.7.2.2) Second order rectangular element	28
	2.7.2.3) Third order rectangular element	29
	2.7.2.4) Analysis steps for 4-noded rectangular element	29
	2.7.2.5) Formulation of element stiffness matrix	32
	2.7.2.6) Load vector due to boundar forces	32
	2.7.2.7) Assembly	33
2.8)	Dynamic analysis	34

		Page
CHAPTER 3:	Solution Covergence	38
3.1)	Static solution	41
	3.1.1) Theoretical solution	41
	3.1.2) NASTRAN solutions	43
	3.1.2.1) According to element's type	43
	3.1.2.2) Structure modelling	46
	3.1.3) Comments	47
3.2)	Dynamic solution	47
	3.2.1) Theoretical solution	48
	3.2.2) NASTRAN solutions	50
3.3)	Conclusion	53
CHAPTER 4:	Results and Discussion	55
4.1)	Static Analysis	55
	4.1.1) The effect of cantilever depth inside the joint casing	58
	4.1.2) Joint casing geometrical effect	64
	4.1.2.1) Effect of case tapering	64
	4.1.2.2) Circular cross-sectional casing effect	70
	4.1.3) The effect of the surface waviness	74
	4.1.4) The adhesive fillet effect	83
	4.1.5) Adhesive back side effect	87
	4.1.6) Bonding of dissimilar materials	89
	4.1.7) The stress distribution across the adhesive thickness	97
	4.1.8) The stress transmission across the adhesive	99
	4.1.9) Comparison in the stress distribution between bonded and solid joints.	105
	4.1.10) The stress distribution across the adhesive section	107
	4.1.11) The Load Magnitude Effect	112
	4.1.12) General discussion and conclusions	114
4.2)	Dynamic Analysis	118
	4.2.1) Effect of the beam depth inside the joint casing	119
	4.2.1.1) Effect on the natural frequencies	119
	4.2.1.2) Effect on the deflection	120
	4.2.1.3) Effect on stresses	121
	4.2.2) Tapering of the joint casing	122
	4.2.2.1) Effect on the natural frequencies	122
	4.2.2.2) Effect on the deflection	123
	4.2.2.3) Effect on stresses	124
	4.2.3) Adhesive surface waviness	125
	4.2.3.1) Effect on the natural frequencies	125
	4.2.3.2) Effect on the deflection	126
	4.2.3.3) Effect on stresses	127

Page

4.2.4) Adhesive fillet effect 128
4.2.4.1) Effect on the natural frequencies 128
4.2.4.2) Effect on the deflection 130
4.2.4.3) Effect on stresses 130
4.2.5) Joint casing clamping effect 132
4.2.5.1) Effect on the natural frequencies 132
4.2.5.2) Effect on the deflection 135
4.2.5.3) Effect on stresses 135
4.2.6) Bonding of dissimilar adherends 137
4.2.6.1) Effect on natural frequencies 137
4.2.6.2) Effect on the deflection 142
4.2.6.3) Effect on stresses 142
4.2.7) General discussion and conclusions 144

Conclusions 146

REFERENCES 148

TABLES

FIGURES

CURVES

NOTATION

d	Lap joint eccentricity distance
P or F	Applied load
R	Region of domain
B	Boundary
x	Any point in the region R
$E(x)$	Exact response or solution to a given point
$L(E)$	Governing differential equations
$B(E)$	Known boundary conditions
$\phi_i(x)$	Coordinate function at i point
$F(x,A)$	Exact response or solution to a given point
r	Arbitrary point in the region
P	Arbitrary point on the boundary
n	The summation of the arbitrary points r and p
$\{F\}$	Trial function or load vector
$[N]$	Coordinate function at i point; called shape function
$\{\delta\}^e$	Nodal displacement at i point
$\{\varepsilon\}$	Normal strain vector
$[B]$	Strain-displacement transformation matrix
$\{\sigma\}$	Stress matrix
$[D]$	Elasticity matrix
π_i	Total potential energy
$[K]$	Stiffness matrix
W_j	Weightage function
n	Number of degrees of freedom
NB	Bandwidth
NDoF	Kinematic degrees of freedom, defined in NASTRAN as follows: 1: Displacement in x-direction 2: Displacement in y-direction 3: Displacement in z-direction 4: Rotation around x-axis 5: Rotation around y-axis 6: Rotation around z-axis
E	Material modulus of elasticity
I	Moment of inertia
h	Distance between subsequent nodes
x	Cartesian coordinate
y	Cartesian coordinate
z	Cartesian coordinate, cylindrical coordinate
y_i	Nodal displacement in y-direction
M	Moment
η	Length ratio of element
ξ	Length ratio of element
q	Local coordinate
r	Local coordinate
L_i	Area coordinate
A_i	Element area

$\{e\}^T$	Thermal strain
$\{\varepsilon\}^T$	Thermal strain
$\{\xi\}^T$	Thermal strain
α	Coefficient of thermal expansion
δT	Temperature change
μ or ν	Poisson's ratio
u, v, w	Displacements corresponding to x, y, z or r, z, o directions
U, V, W	Displacement component of each point
B_x, B_y	Body force component in x, y direction (load/volume)
P_x, P_y	Boundary force components in x, y directions (load/unit length)
h	Thickness
Σ	Summation sign
$[DB]$	Stree-displacement matrix
G	Shear modulus
γ	Shear Strain
σ	Normal Stress
τ	Shear Stress
ϕ	Principal angle
τ_{max}	Maximum shear stress
L	Total length of the bond side under consideration
x/L	The nondimensional distance along adhesive or adherend
w	The domain deflection
au1	Adhesive upper side adjacent to the joint casing
au3	Adhesive upper central side
au5	Adhesive upper side adjacent to the joint beam
al1	Adhesive lower side adjacent to the joint beam
al3	Adhesive lower central side
al5	Adhesive lower side adjacent to the joint casing
ab1	Adhesive back side adjacent to joint casing
ab3	Adhesive back central side
ab5	Adhesive back side adjacent to the left side of the joint beam
c1	Casing upper surface
c2	Casing surface adjacent to the adhesive upper side
c3	Casing surface adjacent to the adhesive back side
c4	Casing surface adjacent to the adhesive lower side
c5	Casing lower surface
c6	Casing back surface
a1	Cantilever surface adjacent to the adhesive upper side
a2	Cantilever surface adjacent to the adhesive back side
a3	Cantilever surface adjacent to the adhesive lower side

Subscripts:-

x,y,z	Refer to directions of stresses and strains in cartesian coordinates
1,2	Refer to major and minor stresses, respectively

Dynamic Symbols

$[M]$	Mass matrix
$[C]$	Damping matrix
$[K]$	Stiffness matrix
$[D]$	Displacement matrix
$[\dot{D}]$	Velocity matrix
$[\ddot{D}]$	Acceleration matrix
$\{R\}$	Generalized forces applied to nodes corresponding to {D}
$\{f_i\}$	Displacement of each element
$\{\dot{f}\}$	Velocity of each element
$[N]$	Shape function matrix
ρ	Material density
T	Total kinetic energy of the structure
F	Dissipative forces
ω	Eigenvalue
ω_i	System i-th natural frequency (rad/sec)
λ	The squared eigenvalue
$[I]$	Unit matrix
$[A]$	Symmetric matrix
$\{Y\}$	Trial vector
Δt	Time step
Λ	The shifted eigenvalue
γ	Constant
β	Constant
f_i	System i-th natural frequency (cycle/sec)
π	Constant = 3.147
A_i	The i-th amplitude of the system with respect to fi
$\{U\}$	The displacement vector
m	Mass density of the beam per unit length
$\phi_n(x)$	The characteristic function of the n-th mode
$T1$	The elastic curve in the x-direction with respect to free vibration
$T2$	The elastic curve in the y-direction with respect to free vibration

List of Tables

3.1) Cantilever conditions summary
3.2) Cantilever conditions summary
3.3) Cantilever conditions summary
3.4) Cantilever conditions summary
3.5) Natural frequency for clamped - clamped beam
3.6) Natural frequency % error
3.8) Natural frequency % error
3.9) Natural frequency % error
3.10) Natural frequency % error
4.1) Material properties
4.2) Cantilever depth % inside the casing
4.3) Zero stress point location
4.4) Stress magnitudes along the adhesive upper side
4.5) Stress magnitudes of circular casing joints
4.6) Adhesive thickness schedule
4.7) Adhesive thickness schedule
4.8) The fillet dimensions of joints in fig. 4.15
4.9) Stress magnitude at X/L = 100% of adhesive upper side
4.10) The fillet dimensions of joints in figs. 4.16 and 4.*.9.a
4.11) The fillet dimensions of joints in figs. 4.17 and 4.*.9.b
4.12) Stress ranges along adhesive upper side
4.13) Material composition of the double containment joint
4.14) Material composition of the double containment joint (with a fillet)
4.15) Material composition of the double containment joint.
4.16) Adhesive back side stress comparison between fully and back clamped joints
4.17) Material composition of a joint
4.18) Material composition of a double strap joint
4.19) Material composition of a double strap joint
4.20) Beam depth % inside the joint casing
4.21) Joint natural frequency
4.22) Joint natural frequency
4.23) Natural frequency ratios for back clamped joint
4.24) Adhesive thickness of the double containment joint
4.25) Natural frequency ratios
4.26) The fillet size of a joint
4.27) Natural frequency ratios for fully clamped joint
4.28) Joint method of clamping description
4.29) Frequency ratios for joints with different methods of clamping
4.30) Joint method of clamping description of a double containment joint with fillet 5x5 mm
4.31) Joint method of clamping description of a scarfed double containment joint
4.32) Normal modes for joints with different clamping of joints with fillets
4.33) Normal modes for joints with different clamping of scarfed joints
4.34) Joint description (refer to fig. 4.*.26.a)
4.35) Joint description (refer to fig. 4.*.26.b)
4.36) Joint description (refer to fig. 4.*.26.c)
4.37) Joint description (refer to fig. 4.*.26.d)
4.38) Natural frequency ratios
4.39) Natural frequency ratios
4.40) Natural frequency ratios
4.41) Natural frequency ratios

List of Figures

1.1) The eccentricity of the load path in a lap joint
1.2) Shape functions and weight functions
1.3) The stress distribution is a lap joint
1.4) The stress distribution along the overlap line of a lap joint
1.5) The bonded double containment joint mesh configuration
1.6) The load case of a double containment joint
2.1) Region of domain
2.2) Finite element mesh
2.3) Domain
2.4) Beam nodes distribution
2.5) Global coordinate system
2.6) Natural coordinate system
2.7) Triangular element
2.8) Triangular element area coordinate
2.9) Stress - strain three - dimensional coordinate
2.10) Thin body in a state of plane stress
2.11) Double containment joint plane stress state
2.12) Coordinate system
2.13) Shape factor
2.14) Coordinate system
2.15) Third order rectangular element
2.16) System coordinate
2.17) The double containment joint representation
2.18) Coordinate system
2.19) Double containment joint with metal to metal contact
3.*.1) MSC/NASTRAN DATA DECK
3.*.2) Schematic of NASTRAN Functional Organization
3.*.3) Prismatic body stress distribution
3.*.4) Cantilever beam
3.*.5) Cantilever beam dimensions
3.*.6) Stress distribution at a section
3.*.7) Cantilever beam
3.*.8) Beam different method of clamping
3.*.9) Finite element mesh configuration of the bonded joint
3.*.10) Finite element mesh patterns
3.*.11) Cantilever boundary conditions
3.*.12) Cantilever beam boundary condition
3.*.13) Cantilever beam boundary condition
3.*.14) Cantilever beam boundary condition
4.*.1) Typical bonded double containment joint
4.*.2) Finite element mesh configuration of the adhesive sides
4.*.3) Finite element mesh configuration of the joint
4.*.4) Back clamped double containment joint
4.*.5) A double containment joint with tapered casing
4.*.6) Scarfed double containment joint
4.*.7) Dimensions of the tapered double containment joint
4.*.8) Double strap joint configuration
4.*.9) The tapered double strap joint configuration
4.*.10) The circular cross-sectional casing joint configuration
4.*.11) Different surface waviness profiles of bonded joints
4.*.12) Different surface waviness profiles of bonded joints

4.*.13) Fillet configuration of the double containment joints
4.*.14) Fillet configuration of the double containment joints
4.*.15) Adhesive deflection in existence of back air gap
4.*.16) Adhesive sublayers notations
4.*.17) Scarfed double containment joint configuration
4.*.18) Stress distribution location of bonded and solid joints
4.*.19) Joints configuration
4.*.20) Various modes of failure
4.*.21) Load location on the joint beam
4.*.22) Joint configuration
4.*.23) The 5-case studies configuration
4.*.24) Joint configuration
4.*.25) Modal shape of a beam fixed from one end
4.*.26) Joint configuration
4.*.27) Optimal design of a double containment joint subjected to static load P
4.*.28) Optimal design of a double containment joint subjected to free vibration
4.*.29) Optimal design of a doule containment joint under static and dynamic considerations

List of Curves

AA) / **Solution Convergence**

Fig. 3.1.a : σ_x vs beam central axis
Fig. 3.1.b : σ_y vs beam central axis
Fig. 3.1.c : τ_{xy} vs beam central axis
Fig. 3.2.a : σ_x vs beam central axis
Fig. 3.2.b : σ_y vs beam central axis
Fig. 3.2.c : τ_{xy} vs beam central axis
Fig. 3.3.a : σ_x vs beam central axis
Fig. 3.3.b : σ_y vs beam central axis
Fig. 3.3.c : τ_{xy} vs beam central axis
Fig. 3.4.a : $\phi_1(x)$ vs beam central axis
Fig. 3.4.b : $\phi_2(x)$ vs beam central axis
Fig. 3.4.c : $\phi_3(x)$ vs beam central axis.
Fig. 3.5.a : $\phi_1(x)$ vs beam central axis
Fig. 3.5.b : $\phi_2(x)$ vs beam central axis
Fig. 3.5.c : $\phi_3(x)$ vs beam central axis

BB) **Static Analysis:**

. The effect of the cantilever depth inside the joint casing

Fig. 4.1. a : σ_x vs X/L along the adhesive upper side
Fig. 4.1. b : σ_y vs X/L along the adhesive upper side
Fig. 4.1. c : ϕ vs X/L along the adhesive upper side
Fig. 4.1. d : σ_1 vs X/L along the adhesive upper side
Fig. 4.1. e : τ_{max} vs X/L along the adhesive upper side
Fig. 4.2. a : σ_x vs X/L along the adhesive back side
Fig. 4.2. b : σ_y vs X/L along the adhesive back side
Fig. 4.2. c : ϕ vs X/L along the adhesive back side
Fig. 4.2. d : σ_1 vs X/L along the adhesive back side
Fig. 4.2. e : τ_{max} vs X/L along the adhesive back side
Fig. 4.3. a : σ_x vs X/L along the adhesive upper side
Fig. 4.3. b . σ_y vs X/L along the adhesive upper side
Fig. 4.3. c : σ_1 vs X/L along the adhesive upper side
Fig. 4.3. d : τ_{max} vs X/L along the adhesive upper side

. Effect of case tapering

Fig. 4.4. a : σ_x vs X/L along the adhesive upper side
Fig. 4.4. b : σ_y vs X/L along the adhesive upper side
Fig. 4.4. c : σ_1 vs X/L along the adhesive upper side
Fig. 4.5. a : σ_x vs X/L along the adhesive upper side
Fig. 4.5. b : σ_y vs X/L along the adhesive upper side
Fig. 4.5. c : σ_1 vs X/L along the adhesive upper side
Fig. 4.5. d : τ_{max} vs X/L along the adhesive upper side
Fig. 4.6. a : σ_x vs X/L along the adhesive upper side
Fig. 4.6. b : σ_y vs X/L along the adhesive upper side
Fig. 4.6. c : σ_1 vs X/L along the adhesive upper side
Fig. 4.6. d : τ_{max} vs X/L along the adhesive upper side
Fig. 4.7. a : σ_x vs X/L along the adhesive upper side
Fig. 4.7. b : σ_y vs X/L along the adhesive upper side

. Circular cross-sectional casing effect

Fig. 4.8. a : σ_x vs X/L along the adhesive upper side
Fig. 4.8. b : σ_y vs X/L along the adhesive upper side
Fig. 4.8. c : τ_{xy} vs X/L along the adhesive upper side
Fig. 4.8. d : ϕ vs X/L along the adhesive upper side
Fig. 4.8. e : σ_1 vs X/L along the adhesive upper side
Fig. 4.9. a : σ_x vs X/L along the adhesive back side
Fig. 4.9. b : σ_y vs X/L along the adhesive back side
Fig. 4.9. c : τ_{xy} vs X/L along the adhesive back side
Fig. 4.9. d : ϕ vs X/L along the adhesive back side
Fig. 4.9. e : σ_1 vs X/L along the adhesive back side

. The effect of the surface waviness

Fig. 4.10.a : σ_x vs X/L along the adhesive upper side
Fig. 4.10.b : σ_y vs X/L along the adhesive upper side
Fig. 4.10.c : τ_{xy} vs X/L along the adhesive upper side
Fig. 4.10.d : ϕ vs X/L along the adhesive upper side
Fig. 4.10.e : σ_1 vs X/L along the adhesive upper side
Fig. 4.11.a : σ_x vs X/L along the adhesive back side
Fig. 4.11.b : σ_y vs X/L along the adhesive back side
Fig. 4.11.c : τ_{xy} vs X/L along the adhesive back side
Fig. 4.11.d : ϕ vs X/L along the adhesive back side
Fig. 4.11.e : σ_1 vs X/L along the adhesive back side
Fig. 4.12.a : σ_x vs X/L along the adhesive upper side
Fig. 4.12.b : σ_y vs X/L along the adhesive upper side
Fig. 4.12.c : τ_{xy} vs X/L along the adhesive upper side
Fig. 4.12.d : ϕ vs X/L along the adhesive upper side
Fig. 4.12.e : σ_1 vs X/L along the adhesive upper side
Fig. 4.13.a : σ_x vs X/L along the adhesive upper side
Fig. 4.13.b : σ_y vs X/L along the adhesive upper side
Fig. 4.13.c : τ_{xy} vs X/L along the adhesive upper side
Fig. 4.13.d : ϕ vs X/L along the adhesive upper side
Fig. 4.13.e : σ_1 vs X/L along the adhesive upper side
Fig. 4.14.a : σ_x vs X/L along the adhesive upper side
Fig. 4.14.b : σ_y vs X/L along the adhesive upper side
Fig. 4.14.c : τ_{xy} vs X/L along the adhesive upper side
Fig. 4.14.d : ϕ vs X/L along the adhesive upper side
Fig. 4.14.e : σ_1 vs X/L along the adhesive upper side

. The adhesive fillet effect

Fig. 4.15.a : σ_x vs X/L along the adhesive upper side
Fig. 4.15.b : σ_y vs X/L along the adhesive upper side
Fig. 4.15.c : τ_{xy} vs X/L along the adhesive upper side
Fig. 4.15.d : ϕ vs X/L along the adhesive upper side
Fig. 4.15.e : σ_1 vs X/L along the adhesive upper side
Fig. 4.16.a : σ_x vs X/L along the adhesive upper side
Fig. 4.16.b : σ_y vs X/L along the adhesive upper side
Fig. 4.16.c : τ_{xy} vs X/L along the adhesive upper side
Fig. 4.16.d : ϕ vs X/L along the adhesive upper side
Fig. 4.16.e : σ_1 vs X/L along the adhesive upper side
Fig. 4.17.a : σ_x vs X/L along the adhesive upper side
Fig. 4.17.b : σ_y vs X/L along the adhesive upper side
Fig. 4.17.c : τ_{xy} vs X/L along the adhesive upper side
Fig. 4.17.d : ϕ vs X/L along the adhesive upper side
Fig. 4.17.e : σ_1 vs X/L along the adhesive upper side

. Adhesive back side effect

Fig. 4.18.a : σ_x vs X/L along the adhesive upper side
Fig. 4.18.b : σ_y vs X/L along the adhesive upper side
Fig. 4.18.c : τ_{xy} vs X/L along the adhesive upper side
Fig. 4.18.d : σ_1 vs X/L along the adhesive upper side
Fig. 4.18.e : τ_{max} vs X/L along the adhesive upper side
Fig. 4.19.a : σ_x vs X/L along the beam depth inside the joint casing
Fig. 4.19.b : σ_y vs X/L along the beam depth inside the joint casing
Fig. 4.19.c : τ_{xy} vs X/L along the beam depth inside the joint casing

. Bonding of dissimilar materials

Fig. 4.20.a : σ_x vs X/L along the adhesive upper side
Fig. 4.20.b : σ_y vs X/L along the adhesive upper side
Fig. 4.20.c : τ_{xy} vs X/L along the adhesive upper side
Fig. 4.20.d : ϕ vs X/L along the adhesive upper side
Fig. 4.20.e : σ_1 vs X/L along the adhesive upper side
Fig. 4.21.a : σ_x vs X/L along the adhesive back side
Fig. 4.21.b : σ_y vs X/L along the adhesive back side
Fig. 4.21.c : τ_{xy} vs X/L along the adhesive back side
Fig. 4.21.d : ϕ vs X/L along the adhesive back side
Fig. 4.21.e : σ_1 vs X/L along the adhesive back side
Fig. 4.22.a : σ_x vs X/L along the adhesive upper side
Fig. 4.22.b : σ_y vs X/L along the adhesive upper side
Fig. 4.22.c : τ_{xy} vs X/L along the adhesive upper side
Fig. 4.22.d : ϕ vs X/L along the adhesive upper side
Fig. 4.22.e : σ_1 vs X/L along the adhesive upper side
Fig. 4.23.a : σ_x vs X/L along the adhesive back side
Fig. 4.23.b : σ_y vs X/L along the adhesive back side
Fig. 4.23.c : τ_{xy} vs X/L along the adhesive back side
Fig. 4.23.d : ϕ vs X/L along the adhesive back side
Fig. 4.23.e : σ_1 vs X/L along the adhesive back side
Fig. 4.24.a : σ_x vs X/L along the adhesive upper side
Fig. 4.24.b : σ_y vs X/L along the adhesive upper side
Fig. 4.24.c : σ_1 vs X/L along the adhesive upper side
Fig. 4.24.d : σ_2 vs X/L along the adhesive upper side
Fig. 4.24.e : τ_{max} vs X/L along the adhesive upper side
Fig. 4.24.f : ϕ vs X/L along the adhesive upper side
Fig. 4.25.a : σ_x vs X/L along the adhesive back side
Fig. 4.25.b : σ_y vs X/L along the adhesive back side
Fig. 4.25.c : σ_1 vs X/L along the adhesive back side
Fig. 4.25.d : σ_2 vs X/L along the adhesive back side
Fig. 4.25.e : τ_{max} vs X/L along the adhesive back side
Fig. 4.25.f : ϕ vs X/L along the adhesive back side

. The stress distribution across the adhesive thickness

Fig. 4.26.a : σ_x vs X/L along the beam depth inside the joint casing
Fig. 4.26.b : σ_y vs X/L along the beam depth inside the joint casing
Fig. 4.26.c : σ_1 vs X/L along the beam depth inside the joint casing
Fig. 4.26.d : τ_{max} vs X/L along the beam depth inside the joint casing
Fig. 4.27.a : σ_x vs X/L along the adhesive back side
Fig. 4.27.b : ϕ vs X/L along the adhesive back side
Fig. 4.27.c : σ_1 vs X/L along the adhesive back side
Fig. 4.27.d : τ_{max} vs X/L along the adhesive back side

. The stress transmission across the adhesive

Fig. 4.28.a : σ_x vs X/L along the outside casing surface
Fig. 4.28.b : σ_y vs X/L along the outside casing surface
Fig. 4.28.c : σ_1 vs X/L along the outside casing surface
Fig. 4.29.a : σ_x vs X/L along the beam depth inside the joint casing
Fig. 4.29.b : σ_y vs X/L along the beam depth inside the joint casing
Fig. 4.29.c : σ_1 vs X/L along the beam depth inside the joint casing
Fig. 4.30.a : σ_x vs X/L along the adherend surface
Fig. 4.30.b : σ_y vs X/L along the adherend surface
Fig. 4.30.c : σ_1 vs X/L along the adherend surface
Fig. 4.31.a : σ_x vs X/L along the beam upper surface inside the casing
Fig. 4.31.b : σ_y vs X/L along the beam upper surface inside the casing
Fig. 4.31.c : σ_1 vs X/L along the beam upper surface inside the casing
Fig. 4.32.a : σ_x vs X/L along the outside casing surface
Fig. 4.32.b : σ_y vs X/L along the outside casing surface
Fig. 4.32.c : σ_1 vs X/L along the outside casing surface
Fig. 4.33.a : σ_x vs X/L along the outside casing surface
Fig. 4.33.b : σ_y vs X/L along the outside casing surface
Fig. 4.33.c : σ_1 vs X/L along the outside casing surface
Fig. 4.34.a : σ_1 vs X/L along the beam depth inside the casing
Fig. 4.34.b : τ_{max} vs X/L along the beam depth inside the casing
Fig. 4.35.a : σ_x σ_1 vs X/L along the adhesive upper side, au1
Fig. 4.35.b : σ_x σ_1 vs X/L along the adhesive upper side, au3
Fig. 4.35.c : σ_x σ_1 vs X/L along the adhesive upper side, au5
Fig. 4.36.a : σ_x σ_1 vs X/L along the adhesive lower side, al1
Fig. 4.36.b : σ_x σ_1 vs X/L along the adhesive lower side, al3
Fig. 4.36.c : σ_x σ_1 vs X/L along the adhesive lower side, al5
Fig. 4.37.a : ϕ vs X/L along the adhesive lower side, al1
Fig. 4.37.b : ϕ vs X/L along the adhesive lower side, al3
Fig. 4.37.c : ϕ vs X/L along the adhesive lower side, al5
Fig. 4.37.d : ϕ vs X/L along the adhesive upper side, au1
Fig. 4.37.e : ϕ vs X/L along the adhesive upper side, au3
Fig. 4.37.f : ϕ vs X/L along the adhesive upper side, au5
Fig. 4.38.a : σ_x vs displacement for adhesive upper and back sides
Fig. 4.38.b : σ_y vs displacement for adhesive upper and back sides
Fig. 4.38.c : σ_1 vs displacement for adhesive upper and back sides

. Comparison in the stress distribution between bonded and solid joints

Fig. 4.39.a : σ_x vs X/L along the adhesive upper side
Fig. 4.39.b : σ_y vs X/L along the adhesive upper side
Fig. 4.39.c : τ_{xy} vs X/L along the adhesive upper side
Fig. 4.39.d : ϕ vs X/L along the adhesive upper side
Fig. 4.39.e : σ_1 vs X/L along the adhesive upper side
Fig. 4.40.a : σ_x vs X/L along the adhesive upper side
Fig. 4.40.b : σ_y vs X/L along the adhesive upper side
Fig. 4.40.c : τ_{xy} vs X/L along the adhesive upper side
Fig. 4.40.d : ϕ vs X/L along the adhesive upper side
Fig. 4.40.e : σ_1 vs X/L along the adhesive upper side
Fig. 4.41.a : σ_x vs X/L along the adhesive upper side
Fig. 4.41.b : σ_y vs X/L along the adhesive upper side

Fig. 4.41.c : τ_{xy} vs X/L along the adhesive upper side
Fig. 4.41.d : ϕ vs X/L along the adhesive upper side
Fig. 4.41.e : σ_1 vs X/L along the adhesive upper side

. The stress distribution across the adhesive section

Fig. 4.42.a : σ_x vs X/L along the adhesive section
Fig. 4.42.b : σ_y vs X/L along the adhesive section
Fig. 4.42.c : τ_{xy} vs X/L along the adhesive section
Fig. 4.42.d : ϕ vs X/L along the adhesive section
Fig. 4.42.e : σ_1 vs X/L along the adhesive section
Fig. 4.42.f : τ_{max} vs X/L along the adhesive section
Fig. 4.43.a : σ_x vs X/L along the adhesive section
Fig. 4.43.b : σ_y vs X/L along the adhesive section
Fig. 4.43.c : ϕ vs X/L along the adhesive section
Fig. 4.43.d : σ_1 vs X/L along the adhesive section
Fig. 4.43.e : τ_{max} vs X/L along the adhesive section

. The load magnitude effect

Fig. 4.44.a : σ_x vs X/L along the adhesive upper side
Fig. 4.44.b : σ_y vs X/L along the adhesive upper side
Fig. 4.44.c : ϕ vs X/L along the adhesive upper side
Fig. 4.44.d : σ_1 vs X/L along the adhesive upper side
Fig. 4.44.e : τ_{max} vs X/L along the adhesive upper side

CC) Dynamic Analysis:

. The effect of the cantilever depth inside the joint casing

Fig. 4.45.a : $\bar{f}$ vs the joint number
Fig. 4.45.b : f vs the joint number
Fig. 4.46.a : $T1$ vs X/L along the beam axis
Fig. 4.46.b : $T2$ vs X/L along the beam axis
Fig. 4.46.c : σ_1 vs X/L along the adhesive upper side
Fig. 4.46.d : ϕ vs X/L along the adhesive upper side
Fig. 4.46.e : τ_{max} vs X/L along the adhesive upper side

. The effect of the joint casing tapering

Fig. 4.47.a : $\bar{f}$ vs the joint number
Fig. 4.47.b : f vs the joint number
Fig. 4.48.a : $T1$ vs X/L along the beam axis
Fig. 4.48.b : $T2$ vs X/L along the beam axis
Fig. 4.48.c : σ_1 vs X/L along the adhesive upper side
Fig. 4.48.d : ϕ vs X/L along the adhesive upper side
Fig. 4.48.e : τ_{max} vs X/L along the adhesive upper side

. The effect of the surface waviness

Fig. 4.49.a : δ vs the joint number
Fig. 4.49.b : δ vs the joint number
Fig. 4.50.a : τ_1 vs X/L along the beam axis
Fig. 4.50.b : τ_2 vs X/L along the beam axis
Fig. 4.50.c : σ_1 vs X/L along the adhesive upper side
Fig. 4.50.d : ϕ vs X/L along the adhesive upper side
Fig. 4.50.e : τ_{max} vs X/L along the adhesive upper side

. The adhesive fillet effect

Fig. 4.51.a : δ vs the joint number
Fig. 4.51.b : δ vs the joint number
Fig. 4.52.a : τ_1 vs X/L along the beam axis
Fig. 4.52.b : τ_2 vs X/L along the beam axis
Fig. 4.52.c : σ_1 vs X/L along the adhesive upper side
Fig. 4.52.d : ϕ vs X/L along the adhesive upper side
Fig. 4.52.e : τ_{max} vs X/L along the adhesive upper side

. The joint casing clamping effect

Fig. 4.53.a : δ vs the joint number
Fig. 4.53.b : δ vs the joint number
Fig. 4.54.a : δ vs the joint number
Fig. 4.54.b : δ vs the joint number
Fig. 4.55.a : δ vs the joint number
Fig. 4.55.b : δ vs the joint number
Fig. 4.56.a : τ_1 vs X/L along the beam axis
Fig. 4.56.b : τ_2 vs X/L along the beam axis
Fig. 4.56.c : σ_1 vs X/L along the adhesive upper side
Fig. 4.56.d : ϕ vs X/L along the adhesive upper side
Fig. 4.56.e : τ_{max} vs X/L along the adhesive upper side

: Bonding of dissimilar adherends

Fig. 4.57.a : δ vs the joint number
Fig. 4.57.b : δ vs the joint number
Fig. 4.58.a : δ vs the joint number
Fig. 4.58.b : δ vs the joint number
Fig. 4.59.a : δ vs the joint number
Fig. 4.59.b : δ vs the joint number
Fig. 4.60.a : δ vs the joint number
Fig. 4.60.b : δ vs the joint number
Fig. 4.61.a : δ vs the joint number
Fig. 4.61.b : δ vs the joint number
Fig. 4.62.a : δ vs the joint number
Fig. 4.62.b : δ vs the joint number
Fig. 4.63.a : δ vs the joint number
Fig. 4.63.b : δ vs the joint number
Fig. 4.64.a : δ vs the joint number
Fig. 4.64.b : δ vs the joint number
Fig. 4.65.a : τ_1 vs X/L along the beam axis

Fig. 4.65.b : T_2 vs X/L along the beam axis
Fig. 4.65.c : σ_1 vs X/L along the adhesive upper side
Fig. 4.65.d : ϕ vs X/L along the adhesive upper side
Fig. 4.65.e : τ_{max} vs X/L along the adhesive upper side

دار المنظومة
DAR ALMANDUMAH
الرواد في قواعد المعلومات العربية

العنوان:	The Investigation of the effect of Various Parameters of Double Containment Joint of a Composite Structure
المؤلف الرئيسي:	Krayyem, Ahmad Mohammed
مؤلفين آخرين:	Sadek, Medhat M.(Super)
التاريخ الميلادي:	1990
موقع:	الكويت
الصفحات:	1 - 466
رقم MD:	586776
نوع المحتوى:	رسائل جامعية
اللغة:	English
الدرجة العلمية:	رسالة ماجستير
الجامعة:	جامعة الكويت
الكلية:	كلية الهندسة
الدولة:	الكويت
قواعد المعلومات:	Dissertations
مواضيع:	الهندسة الميكانيكية، تكنولوجيا التثبيت
رابط:	https://search.mandumah.com/Record/586776

© 2020 دار المنظومة. جميع الحقوق محفوظة.
هذه المادة متاحة بناء على الإتفاق الموقع مع أصحاب حقوق النشر، علما أن جميع حقوق النشر محفوظة. يمكنك تحميل أو طباعة هذه المادة للاستخدام الشخصي فقط، ويمنع النسخ أو التحويل أو النشر عبر أي وسيلة (مثل مواقع الانترنت أو البريد الالكتروني) دون تصريح خطي من أصحاب حقوق النشر أو دار المنظومة.

المنارة للاستشارات
www.manaraa.com

The Investigation of the effect of Various Parameters of Double Containment Joint of a Composite Structure

Prepared by

Ahmad Mohammed Krayyem

Supervised by

Prof. Medhat M Sadek

A Thesis submitted for the Partial fulfillment for the Degree of Master of Science at the University of Kuwait

To my parents and brother Emad for their encouragement and help.

Acknowledgment

This project is a part of a major grant EM023 awarded to Professor M. M. Sadek, Professor in the Mechanical Engineering Department.

The Author wishes his gratitude to Professor M. M. Sadek for his guidance and supervision throughout the work.

Thanks are also due to Professor Farouk Badrakhan for his suggestions and encouragement.

I would also like to extend my thanks to all the staff at the Kuwait University Computer Center for their active cooperation and help.

ABSTRACT

Adhesive bonding added a new dimension to the technology of fastening. The bonding technique was applied successfully in different fields such as aircrafts, workshop machines, e.g.: fully bonded milling machine, and the gear box of a lathe machine, ... etc..

However, no attempts were made on optimizing the various parameters of the joint configuration on the basis of the strength of a double containment joint.

The work reported here is an investigation into the stress distributions in adhesive bonded double containment joint.

It is aimed at improving the joint performance under the static and dynamic loading and to give most possible uniform stress distribution along the adhesive layers, through the change of joint geometry.

A problem usually encountered with bonded joints is the differential straining of the adhesive and adherend materials which causes a state of highly localized stress discountinuity and so causes high stress concentration at the adhesive free edges.

It is shown that Poisson's ratio strains in the adherends of a double containment joint induce tranverse stresses both in the adhesive and in the adherends and so causing the differential straining.

The present investigation is aided by the finite element method using an established program called NASTRAN.

The two-dimensional finite element model (Plain Strain) was used to predict the normal and principal stresses of the bond layers in the static analysis and the natural frequencies of the system in the dynamic one.

The same different joint geometry parameters were investigated for both static and dynamic analyses.

Varying the cantilever depth inside the joint casing was taken as the first parameter of investigation. The results obtained indicated that by increasing the depth of the joint beam the strength increases up to certain limit. While it was found that there is no interpolation between the above parameter and the system natural frequency. The second parameter taken was the joint casing tapering, where it improved the joint strength but it reduced the system natural frequency.

It was found that by increasing the adhesive thickening at the free edge reduces the stress concentration and raises the joint natural frequency.

Real double containment joints, however, are formed with a fillet of adhesive spew, which was represented in the finite element models as a triangular fillet. The presence of the fillet significantly modifies the stress field in the highly-stressed regions at the ends of the overlap.

The significant stresses within the spew are shown to be tensile and at right angles to the direction of cracks. The maximum stress exists at the adherend corner within the fillet, but its value is dependent on the adherend corner shape.

The fillet existence is also recommended in the dynamic case where it raises the natural frequency of the system.

Finally since the adhesive bonding faciliates the joining of dissimilar materials, it is recommended generally to select the joint casing of lower Poisson's ratio than the cantilever.

From the present work an optimal joints were obtained for the static, dynamic and static/ dynamic applications, assuming linearly elastic behavior of the adhesive.

547224

Contents

		Page
Notation		i
List of tables		iv
List of figures		v
List of curves		vii
CHAPTER 1 :	Background and Introductory Material	1
1.1)	Historical review	1
1.2)	Object of the project	5
CHAPTER 2 :	Basis of Finite Element Method	11
2.1)	Introduction	11
2.2)	History	13
2.3)	Basic fundamentals	14
	2.3.1) Typical finite element analysis	14
	2.3.2) Assymbly or system analysis	17
2.4)	"Pseudo" Example of finite elements	19
2.5)	Coordinate systems	21
	2.5.1) Local coordinate systems	21
	2.5.2) Natural coordinate systems	21
	2.5.3) Global coordinate systems	21
	2.5.4) Rectangular element	21
	2.5.5) Triangular element : Area coordinates	22
2.6)	Theory of elasticity	22
	2.6.1) Stress, strain and Hooke's law	23
	2.6.2) The strain-displacements equations	24
	2.6.3) The element matrices	24
	2.6.4) Plane stress and plane strain	24
	2.6.4.1) Plane stress	24
	2.6.4.2) Plane strain	25
2.7)	Element analysis	26
	2.7.1) Shape functions	27
	2.7.2) Rectangular element	27
	2.7.2.1) First order rectangular element	27
	2.7.2.2) Second order rectangular element	28
	2.7.2.3) Third order rectangular element	29
	2.7.2.4) Analysis steps for 4-noded rectangular element	29
	2.7.2.5) Formulation of element stiffness matrix	32
	2.7.2.6) Load vector due to boundar forces	32
	2.7.2.7) Assembly	33
2.8)	Dynamic analysis	34

		Page
CHAPTER 3:	Solution Covergence	38
3.1)	Static solution	41
	3.1.1) Theoretical solution	41
	3.1.2) NASTRAN solutions	43
	3.1.2.1) According to element's type	43
	3.1.2.2) Structure modelling	46
	3.1.3) Comments	47
3.2)	Dynamic solution	47
	3.2.1) Theoretical solution	48
	3.2.2) NASTRAN solutions	50
3.3)	Conclusion	53
CHAPTER 4:	Results and Discussion	55
4.1)	Static Analysis	55
	4.1.1) The effect of cantilever depth inside the joint casing	58
	4.1.2) Joint casing geometrical effect	64
	4.1.2.1) Effect of case tapering	64
	4.1.2.2) Circular cross-sectional casing effect	70
	4.1.3) The effect of the surface waviness	74
	4.1.4) The adhesive fillet effect	83
	4.1.5) Adhesive back side effect	87
	4.1.6) Bonding of dissimilar materials	89
	4.1.7) The stress distribution across the adhesive thickness	97
	4.1.8) The stress transmission across the adhesive	99
	4.1.9) Comparison in the stress distribution between bonded and solid joints.	105
	4.1.10) The stress distribution across the adhesive section	107
	4.1.11) The Load Magnitude Effect	112
	4.1.12) General discussion and conclusions	114
4.2)	Dynamic Analysis	118
	4.2.1) Effect of the beam depth inside the joint casing	119
	4.2.1.1) Effect on the natural frequencies	119
	4.2.1.2) Effect on the deflection	120
	4.2.1.3) Effect on stresses	121
	4.2.2) Tapering of the joint casing	122
	4.2.2.1) Effect on the natural frequencies	122
	4.2.2.2) Effect on the deflection	123
	4.2.2.3) Effect on stresses	124
	4.2.3) Adhesive surface waviness	125
	4.2.3.1) Effect on the natural frequencies	125
	4.2.3.2) Effect on the deflection	126
	4.2.3.3) Effect on stresses	127

Page

4.2.4) Adhesive fillet effect 128
4.2.4.1) Effect on the natural frequencies 128
4.2.4.2) Effect on the deflection 130
4.2.4.3) Effect on stresses 130
4.2.5) Joint casing clamping effect 132
4.2.5.1) Effect on the natural frequencies 132
4.2.5.2) Effect on the deflection 135
4.2.5.3) Effect on stresses 135
4.2.6) Bonding of dissimilar adherends 137
4.2.6.1) Effect on natural frequencies 137
4.2.6.2) Effect on the deflection 142
4.2.6.3) Effect on stresses 142
4.2.7) General discussion and conclusions 144

Conclusions 146

REFERENCES 148

TABLES

FIGURES

CURVES

NOTATION

d	Lap joint eccentricity distance
P or F	Applied load
R	Region of domain
B	Boundary
x	Any point in the region R
$E(x)$	Exact response or solution to a given point
$L(E)$	Governing differential equations
$B(E)$	Known boundary conditions
$\phi_i(x)$	Coordinate function at i point
$F(x,A)$	Exact response or solution to a given point
r	Arbitrary point in the region
P	Arbitrary point on the boundary
n	The summation of the arbitrary points r and p
$\{F\}$	Trial function or load vector
$[N]$	Coordinate function at i point; called shape function
$\{\delta\}^e$	Nodal displacement at i point
$\{\varepsilon\}$	Normal strain vector
$[B]$	Strain-displacement transformation matrix
$\{\sigma\}$	Stress matrix
$[D]$	Elasticity matrix
π_i	Total potential energy
$[K]$	Stiffness matrix
W_j	Weightage function
n	Number of degrees of freedom
NB	Bandwidth
NDoF	Kinematic degrees of freedom, defined in NASTRAN as follows: 1: Displacement in x-direction 2: Displacement in y-direction 3: Displacement in z-direction 4: Rotation around x-axis 5: Rotation around y-axis 6: Rotation around z-axis
E	Material modulus of elasticity
I	Moment of inertia
h	Distance between subsequent nodes
x	Cartesian coordinate
y	Cartesian coordinate
z	Cartesian coordinate, cylindrical coordinate
y_i	Nodal displacement in y-direction
M	Moment
η	Length ratio of element
ξ	Length ratio of element
q	Local coordinate
r	Local coordinate
L_i	Area coordinate
A_i	Element area

$\{e\}^T$	Thermal strain
$\{\varepsilon\}^T$	Thermal strain
$\{\xi\}^T$	Thermal strain
α	Coefficient of thermal expansion
δT	Temperature change
μ or ν	Poisson's ratio
u, v, w	Displacements corresponding to x, y, z or r, z, o directions
U, V, W	Displacement component of each point
B_x, B_y	Body force component in x, y direction (load/volume)
P_x, P_y	Boundary force components in x, y directions (load/unit length)
h	Thickness
Σ	Summation sign
$[DB]$	Stree-displacement matrix
G	Shear modulus
γ	Shear Strain
σ	Normal Stress
τ	Shear Stress
ϕ	Principal angle
τ_{max}	Maximum shear stress
L	Total length of the bond side under consideration
x/L	The nondimensional distance along adhesive or adherend
w	The domain deflection
au1	Adhesive upper side adjacent to the joint casing
au3	Adhesive upper central side
au5	Adhesive upper side adjacent to the joint beam
al1	Adhesive lower side adjacent to the joint beam
al3	Adhesive lower central side
al5	Adhesive lower side adjacent to the joint casing
ab1	Adhesive back side adjacent to joint casing
ab3	Adhesive back central side
ab5	Adhesive back side adjacent to the left side of the joint beam
c1	Casing upper surface
c2	Casing surface adjacent to the adhesive upper side
c3	Casing surface adjacent to the adhesive back side
c4	Casing surface adjacent to the adhesive lower side
c5	Casing lower surface
c6	Casing back surface
a1	Cantilever surface adjacent to the adhesive upper side
a2	Cantilever surface adjacent to the adhesive back side
a3	Cantilever surface adjacent to the adhesive lower side

Subscripts:-

x,y,z	Refer to directions of stresses and strains in cartesian coordinates
1,2	Refer to major and minor stresses, respectively

Dynamic Symbols

$[M]$	Mass matrix
$[C]$	Damping matrix
$[K]$	Stiffness matrix
$[D]$	Displacement matrix
$[\dot{D}]$	Velocity matrix
$[\ddot{D}]$	Acceleration matrix
$\{R\}$	Generalized forces applied to nodes corresponding to {D}
$\{f_i\}$	Displacement of each element
$\{\dot{f}\}$	Velocity of each element
$[N]$	Shape function matrix
ρ	Material density
T	Total kinetic energy of the structure
F	Dissipative forces
ω	Eigenvalue
ω_i	System i-th natural frequency (rad/sec)
λ	The squared eigenvalue
$[I]$	Unit matrix
$[A]$	Symmetric matrix
$\{Y\}$	Trial vector
Δt	Time step
Λ	The shifted eigenvalue
γ	Constant
β	Constant
f_i	System i-th natural frequency (cycle/sec)
π	Constant = 3.147
A_i	The i-th amplitude of the system with respect to fi
$\{U\}$	The displacement vector
m	Mass density of the beam per unit length
$\phi_n(x)$	The characteristic function of the n-th mode
$T1$	The elastic curve in the x-direction with respect to free vibration
$T2$	The elastic curve in the y-direction with respect to free vibration

List of Tables

3.1) Cantilever conditions summary
3.2) Cantilever conditions summary
3.3) Cantilever conditions summary
3.4) Cantilever conditions summary
3.5) Natural frequency for clamped - clamped beam
3.6) Natural frequency % error
3.8) Natural frequency % error
3.9) Natural frequency % error
3.10) Natural frequency % error
4.1) Material properties
4.2) Cantilever depth % inside the casing
4.3) Zero stress point location
4.4) Stress magnitudes along the adhesive upper side
4.5) Stress magnitudes of circular casing joints
4.6) Adhesive thickness schedule
4.7) Adhesive thickness schedule
4.8) The fillet dimensions of joints in fig. 4.15
4.9) Stress magnitude at X/L = 100% of adhesive upper side
4.10) The fillet dimensions of joints in figs. 4.16 and 4.*.9.a
4.11) The fillet dimensions of joints in figs. 4.17 and 4.*.9.b
4.12) Stress ranges along adhesive upper side
4.13) Material composition of the double containment joint
4.14) Material composition of the double containment joint (with a fillet)
4.15) Material composition of the double containment joint.
4.16) Adhesive back side stress comparison between fully and back clamped joints
4.17) Material composition of a joint
4.18) Material composition of a double strap joint
4.19) Material composition of a double strap joint
4.20) Beam depth % inside the joint casing
4.21) Joint natural frequency
4.22) Joint natural frequency
4.23) Natural frequency ratios for back clamped joint
4.24) Adhesive thickness of the double containment joint
4.25) Natural frequency ratios
4.26) The fillet size of a joint
4.27) Natural frequency ratios for fully clamped joint
4.28) Joint method of clamping description
4.29) Frequency ratios for joints with different methods of clamping
4.30) Joint method of clamping description of a double containment joint with fillet 5x5 mm
4.31) Joint method of clamping description of a scarfed double containment joint
4.32) Normal modes for joints with different clamping of joints with fillets
4.33) Normal modes for joints with different clamping of scarfed joints
4.34) Joint description (refer to fig. 4.*.26.a)
4.35) Joint description (refer to fig. 4.*.26.b)
4.36) Joint description (refer to fig. 4.*.26.c)
4.37) Joint description (refer to fig. 4.*.26.d)
4.38) Natural frequency ratios
4.39) Natural frequency ratios
4.40) Natural frequency ratios
4.41) Natural frequency ratios

List of Figures

1.1) The eccentricity of the load path in a lap joint
1.2) Shape functions and weight functions
1.3) The stress distribution is a lap joint
1.4) The stress distribution along the overlap line of a lap joint
1.5) The bonded double containment joint mesh configuration
1.6) The load case of a double containment joint
2.1) Region of domain
2.2) Finite element mesh
2.3) Domain
2.4) Beam nodes distribution
2.5) Global coordinate system
2.6) Natural coordinate system
2.7) Triangular element
2.8) Triangular element area coordinate
2.9) Stress - strain three - dimensional coordinate
2.10) Thin body in a state of plane stress
2.11) Double containment joint plane stress state
2.12) Coordinate system
2.13) Shape factor
2.14) Coordinate system
2.15) Third order rectangular element
2.16) System coordinate
2.17) The double containment joint representation
2.18) Coordinate system
2.19) Double containment joint with metal to metal contact
3.*.1) MSC/NASTRAN DATA DECK
3.*.2) Schematic of NASTRAN Functional Organization
3.*.3) Prismatic body stress distribution
3.*.4) Cantilever beam
3.*.5) Cantilever beam dimensions
3.*.6) Stress distribution at a section
3.*.7) Cantilever beam
3.*.8) Beam different method of clamping
3.*.9) Finite element mesh configuration of the bonded joint
3.*.10) Finite element mesh patterns
3.*.11) Cantilever boundary conditions
3.*.12) Cantilever beam boundary condition
3.*.13) Cantilever beam boundary condition
3.*.14) Cantilever beam boundary condition
4.*.1) Typical bonded double containment joint
4.*.2) Finite element mesh configuration of the adhesive sides
4.*.3) Finite element mesh configuration of the joint
4.*.4) Back clamped double containment joint
4.*.5) A double containment joint with tapered casing
4.*.6) Scarfed double containment joint
4.*.7) Dimensions of the tapered double containment joint
4.*.8) Double strap joint configuration
4.*.9) The tapered double strap joint configuration
4.*.10) The circular cross-sectional casing joint configuration
4.*.11) Different surface waviness profiles of bonded joints
4.*.12) Different surface waviness profiles of bonded joints

4.*.13) Fillet configuration of the double containment joints
4.*.14) Fillet configuration of the double containment joints
4.*.15) Adhesive deflection in existence of back air gap
4.*.16) Adhesive sublayers notations
4.*.17) Scarfed double containment joint configuration
4.*.18) Stress distribution location of bonded and solid joints
4.*.19) Joints configuration
4.*.20) Various modes of failure
4.*.21) Load location on the joint beam
4.*.22) Joint configuration
4.*.23) The 5-case studies configuration
4.*.24) Joint configuration
4.*.25) Modal shape of a beam fixed from one end
4.*.26) Joint configuration
4.*.27) Optimal design of a double containment joint subjected to static load P
4.*.28) Optimal design of a double containment joint subjected to free vibration
4.*.29) Optimal design of a doule containment joint under static and dynamic considerations

List of Curves

AA) / **Solution Convergence**

Fig. 3.1.a : σ_x vs beam central axis
Fig. 3.1.b : σ_y vs beam central axis
Fig. 3.1.c : τ_{xy} vs beam central axis
Fig. 3.2.a : σ_x vs beam central axis
Fig. 3.2.b : σ_y vs beam central axis
Fig. 3.2.c : τ_{xy} vs beam central axis
Fig. 3.3.a : σ_x vs beam central axis
Fig. 3.3.b : σ_y vs beam central axis
Fig. 3.3.c : τ_{xy} vs beam central axis
Fig. 3.4.a : $\phi_1(x)$ vs beam central axis
Fig. 3.4.b : $\phi_2(x)$ vs beam central axis
Fig. 3.4.c : $\phi_3(x)$ vs beam central axis.
Fig. 3.5.a : $\phi_1(x)$ vs beam central axis
Fig. 3.5.b : $\phi_2(x)$ vs beam central axis
Fig. 3.5.c : $\phi_3(x)$ vs beam central axis

BB) **Static Analysis:**

. The effect of the cantilever depth inside the joint casing

Fig. 4.1. a : σ_x vs X/L along the adhesive upper side
Fig. 4.1. b : σ_y vs X/L along the adhesive upper side
Fig. 4.1. c : ϕ vs X/L along the adhesive upper side
Fig. 4.1. d : σ_1 vs X/L along the adhesive upper side
Fig. 4.1. e : τ_{max} vs X/L along the adhesive upper side
Fig. 4.2. a : σ_x vs X/L along the adhesive back side
Fig. 4.2. b : σ_y vs X/L along the adhesive back side
Fig. 4.2. c : ϕ vs X/L along the adhesive back side
Fig. 4.2. d : σ_1 vs X/L along the adhesive back side
Fig. 4.2. e : τ_{max} vs X/L along the adhesive back side
Fig. 4.3. a : σ_x vs X/L along the adhesive upper side
Fig. 4.3. b . σ_y vs X/L along the adhesive upper side
Fig. 4.3. c : σ_1 vs X/L along the adhesive upper side
Fig. 4.3. d : τ_{max} vs X/L along the adhesive upper side

. Effect of case tapering

Fig. 4.4. a : σ_x vs X/L along the adhesive upper side
Fig. 4.4. b : σ_y vs X/L along the adhesive upper side
Fig. 4.4. c : σ_1 vs X/L along the adhesive upper side
Fig. 4.5. a : σ_x vs X/L along the adhesive upper side
Fig. 4.5. b : σ_y vs X/L along the adhesive upper side
Fig. 4.5. c : σ_1 vs X/L along the adhesive upper side
Fig. 4.5. d : τ_{max} vs X/L along the adhesive upper side
Fig. 4.6. a : σ_x vs X/L along the adhesive upper side
Fig. 4.6. b : σ_y vs X/L along the adhesive upper side
Fig. 4.6. c : σ_1 vs X/L along the adhesive upper side
Fig. 4.6. d : τ_{max} vs X/L along the adhesive upper side
Fig. 4.7. a : σ_x vs X/L along the adhesive upper side
Fig. 4.7. b : σ_y vs X/L along the adhesive upper side

. Circular cross-sectional casing effect

Fig. 4.8. a : σ_x vs X/L along the adhesive upper side
Fig. 4.8. b : σ_y vs X/L along the adhesive upper side
Fig. 4.8. c : τ_{xy} vs X/L along the adhesive upper side
Fig. 4.8. d : ϕ vs X/L along the adhesive upper side
Fig. 4.8. e : σ_1 vs X/L along the adhesive upper side
Fig. 4.9. a : σ_x vs X/L along the adhesive back side
Fig. 4.9. b : σ_y vs X/L along the adhesive back side
Fig. 4.9. c : τ_{xy} vs X/L along the adhesive back side
Fig. 4.9. d : ϕ vs X/L along the adhesive back side
Fig. 4.9. e : σ_1 vs X/L along the adhesive back side

. The effect of the surface waviness

Fig. 4.10.a : σ_x vs X/L along the adhesive upper side
Fig. 4.10.b : σ_y vs X/L along the adhesive upper side
Fig. 4.10.c : τ_{xy} vs X/L along the adhesive upper side
Fig. 4.10.d : ϕ vs X/L along the adhesive upper side
Fig. 4.10.e : σ_1 vs X/L along the adhesive upper side
Fig. 4.11.a : σ_x vs X/L along the adhesive back side
Fig. 4.11.b : σ_y vs X/L along the adhesive back side
Fig. 4.11.c : τ_{xy} vs X/L along the adhesive back side
Fig. 4.11.d : ϕ vs X/L along the adhesive back side
Fig. 4.11.e : σ_1 vs X/L along the adhesive back side
Fig. 4.12.a : σ_x vs X/L along the adhesive upper side
Fig. 4.12.b : σ_y vs X/L along the adhesive upper side
Fig. 4.12.c : τ_{xy} vs X/L along the adhesive upper side
Fig. 4.12.d : ϕ vs X/L along the adhesive upper side
Fig. 4.12.e : σ_1 vs X/L along the adhesive upper side
Fig. 4.13.a : σ_x vs X/L along the adhesive upper side
Fig. 4.13.b : σ_y vs X/L along the adhesive upper side
Fig. 4.13.c : τ_{xy} vs X/L along the adhesive upper side
Fig. 4.13.d : ϕ vs X/L along the adhesive upper side
Fig. 4.13.e : σ_1 vs X/L along the adhesive upper side
Fig. 4.14.a : σ_x vs X/L along the adhesive upper side
Fig. 4.14.b : σ_y vs X/L along the adhesive upper side
Fig. 4.14.c : τ_{xy} vs X/L along the adhesive upper side
Fig. 4.14.d : ϕ vs X/L along the adhesive upper side
Fig. 4.14.e : σ_1 vs X/L along the adhesive upper side

. The adhesive fillet effect

Fig. 4.15.a : σ_x vs X/L along the adhesive upper side
Fig. 4.15.b : σ_y vs X/L along the adhesive upper side
Fig. 4.15.c : τ_{xy} vs X/L along the adhesive upper side
Fig. 4.15.d : ϕ vs X/L along the adhesive upper side
Fig. 4.15.e : σ_1 vs X/L along the adhesive upper side
Fig. 4.16.a : σ_x vs X/L along the adhesive upper side
Fig. 4.16.b : σ_y vs X/L along the adhesive upper side
Fig. 4.16.c : τ_{xy} vs X/L along the adhesive upper side
Fig. 4.16.d : ϕ vs X/L along the adhesive upper side
Fig. 4.16.e : σ_1 vs X/L along the adhesive upper side
Fig. 4.17.a : σ_x vs X/L along the adhesive upper side
Fig. 4.17.b : σ_y vs X/L along the adhesive upper side
Fig. 4.17.c : τ_{xy} vs X/L along the adhesive upper side
Fig. 4.17.d : ϕ vs X/L along the adhesive upper side
Fig. 4.17.e : σ_1 vs X/L along the adhesive upper side

. Adhesive back side effect

Fig. 4.18.a : σ_x vs X/L along the adhesive upper side
Fig. 4.18.b : σ_y vs X/L along the adhesive upper side
Fig. 4.18.c : τ_{xy} vs X/L along the adhesive upper side
Fig. 4.18.d : σ_1 vs X/L along the adhesive upper side
Fig. 4.18.e : τ_{max} vs X/L along the adhesive upper side
Fig. 4.19.a : σ_x vs X/L along the beam depth inside the joint casing
Fig. 4.19.b : σ_y vs X/L along the beam depth inside the joint casing
Fig. 4.19.c : τ_{xy} vs X/L along the beam depth inside the joint casing

. Bonding of dissimilar materials

Fig. 4.20.a : σ_x vs X/L along the adhesive upper side
Fig. 4.20.b : σ_y vs X/L along the adhesive upper side
Fig. 4.20.c : τ_{xy} vs X/L along the adhesive upper side
Fig. 4.20.d : ϕ vs X/L along the adhesive upper side
Fig. 4.20.e : σ_1 vs X/L along the adhesive upper side
Fig. 4.21.a : σ_x vs X/L along the adhesive back side
Fig. 4.21.b : σ_y vs X/L along the adhesive back side
Fig. 4.21.c : τ_{xy} vs X/L along the adhesive back side
Fig. 4.21.d : ϕ vs X/L along the adhesive back side
Fig. 4.21.e : σ_1 vs X/L along the adhesive back side
Fig. 4.22.a : σ_x vs X/L along the adhesive upper side
Fig. 4.22.b : σ_y vs X/L along the adhesive upper side
Fig. 4.22.c : τ_{xy} vs X/L along the adhesive upper side
Fig. 4.22.d : ϕ vs X/L along the adhesive upper side
Fig. 4.22.e : σ_1 vs X/L along the adhesive upper side
Fig. 4.23.a : σ_x vs X/L along the adhesive back side
Fig. 4.23.b : σ_y vs X/L along the adhesive back side
Fig. 4.23.c : τ_{xy} vs X/L along the adhesive back side
Fig. 4.23.d : ϕ vs X/L along the adhesive back side
Fig. 4.23.e : σ_1 vs X/L along the adhesive back side
Fig. 4.24.a : σ_x vs X/L along the adhesive upper side
Fig. 4.24.b : σ_y vs X/L along the adhesive upper side
Fig. 4.24.c : σ_1 vs X/L along the adhesive upper side
Fig. 4.24.d : σ_2 vs X/L along the adhesive upper side
Fig. 4.24.e : τ_{max} vs X/L along the adhesive upper side
Fig. 4.24.f : ϕ vs X/L along the adhesive upper side
Fig. 4.25.a : σ_x vs X/L along the adhesive back side
Fig. 4.25.b : σ_y vs X/L along the adhesive back side
Fig. 4.25.c : σ_1 vs X/L along the adhesive back side
Fig. 4.25.d : σ_2 vs X/L along the adhesive back side
Fig. 4.25.e : τ_{max} vs X/L along the adhesive back side
Fig. 4.25.f : ϕ vs X/L along the adhesive back side

. The stress distribution across the adhesive thickness

Fig. 4.26.a : σ_x vs X/L along the beam depth inside the joint casing
Fig. 4.26.b : σ_y vs X/L along the beam depth inside the joint casing
Fig. 4.26.c : σ_1 vs X/L along the beam depth inside the joint casing
Fig. 4.26.d : τ_{max} vs X/L along the beam depth inside the joint casing
Fig. 4.27.a : σ_x vs X/L along the adhesive back side
Fig. 4.27.b : ϕ vs X/L along the adhesive back side
Fig. 4.27.c : σ_1 vs X/L along the adhesive back side
Fig. 4.27.d : τ_{max} vs X/L along the adhesive back side

. The stress transmission across the adhesive

Fig. 4.28.a : σ_x vs X/L along the outside casing surface
Fig. 4.28.b : σ_y vs X/L along the outside casing surface
Fig. 4.28.c : σ_1 vs X/L along the outside casing surface
Fig. 4.29.a : σ_x vs X/L along the beam depth inside the joint casing
Fig. 4.29.b : σ_y vs X/L along the beam depth inside the joint casing
Fig. 4.29.c : σ_1 vs X/L along the beam depth inside the joint casing
Fig. 4.30.a : σ_x vs X/L along the adherend surface
Fig. 4.30.b : σ_y vs X/L along the adherend surface
Fig. 4.30.c : σ_1 vs X/L along the adherend surface
Fig. 4.31.a : σ_x vs X/L along the beam upper surface inside the casing
Fig. 4.31.b : σ_y vs X/L along the beam upper surface inside the casing
Fig. 4.31.c : σ_1 vs X/L along the beam upper surface inside the casing
Fig. 4.32.a : σ_x vs X/L along the outside casing surface
Fig. 4.32.b : σ_y vs X/L along the outside casing surface
Fig. 4.32.c : σ_1 vs X/L along the outside casing surface
Fig. 4.33.a : σ_x vs X/L along the outside casing surface
Fig. 4.33.b : σ_y vs X/L along the outside casing surface
Fig. 4.33.c : σ_1 vs X/L along the outside casing surface
Fig. 4.34.a : σ_1 vs X/L along the beam depth inside the casing
Fig. 4.34.b : τ_{max} vs X/L along the beam depth inside the casing
Fig. 4.35.a : σ_x σ_1 vs X/L along the adhesive upper side, au1
Fig. 4.35.b : σ_x σ_1 vs X/L along the adhesive upper side, au3
Fig. 4.35.c : σ_x σ_1 vs X/L along the adhesive upper side, au5
Fig. 4.36.a : σ_x σ_1 vs X/L along the adhesive lower side, al1
Fig. 4.36.b : σ_x σ_1 vs X/L along the adhesive lower side, al3
Fig. 4.36.c : σ_x σ_1 vs X/L along the adhesive lower side, al5
Fig. 4.37.a : ϕ vs X/L along the adhesive lower side, al1
Fig. 4.37.b : ϕ vs X/L along the adhesive lower side, al3
Fig. 4.37.c : ϕ vs X/L along the adhesive lower side, al5
Fig. 4.37.d : ϕ vs X/L along the adhesive upper side, au1
Fig. 4.37.e : ϕ vs X/L along the adhesive upper side, au3
Fig. 4.37.f : ϕ vs X/L along the adhesive upper side, au5
Fig. 4.38.a : σ_x vs displacement for adhesive upper and back sides
Fig. 4.38.b : σ_y vs displacement for adhesive upper and back sides
Fig. 4.38.c : σ_1 vs displacement for adhesive upper and back sides

. Comparison in the stress distribution between bonded and solid joints

Fig. 4.39.a : σ_x vs X/L along the adhesive upper side
Fig. 4.39.b : σ_y vs X/L along the adhesive upper side
Fig. 4.39.c : τ_{xy} vs X/L along the adhesive upper side
Fig. 4.39.d : ϕ vs X/L along the adhesive upper side
Fig. 4.39.e : σ_1 vs X/L along the adhesive upper side
Fig. 4.40.a : σ_x vs X/L along the adhesive upper side
Fig. 4.40.b : σ_y vs X/L along the adhesive upper side
Fig. 4.40.c : τ_{xy} vs X/L along the adhesive upper side
Fig. 4.40.d : ϕ vs X/L along the adhesive upper side
Fig. 4.40.e : σ_1 vs X/L along the adhesive upper side
Fig. 4.41.a : σ_x vs X/L along the adhesive upper side
Fig. 4.41.b : σ_y vs X/L along the adhesive upper side

Fig. 4.41.c : τ_{xy} vs X/L along the adhesive upper side
Fig. 4.41.d : ϕ vs X/L along the adhesive upper side
Fig. 4.41.e : σ_1 vs X/L along the adhesive upper side

. The stress distribution across the adhesive section

Fig. 4.42.a : σ_x vs X/L along the adhesive section
Fig. 4.42.b : σ_y vs X/L along the adhesive section
Fig. 4.42.c : τ_{xy} vs X/L along the adhesive section
Fig. 4.42.d : ϕ vs X/L along the adhesive section
Fig. 4.42.e : σ_1 vs X/L along the adhesive section
Fig. 4.42.f : τ_{max} vs X/L along the adhesive section
Fig. 4.43.a : σ_x vs X/L along the adhesive section
Fig. 4.43.b : σ_y vs X/L along the adhesive section
Fig. 4.43.c : ϕ vs X/L along the adhesive section
Fig. 4.43.d : σ_1 vs X/L along the adhesive section
Fig. 4.43.e : τ_{max} vs X/L along the adhesive section

. The load magnitude effect

Fig. 4.44.a : σ_x vs X/L along the adhesive upper side
Fig. 4.44.b : σ_y vs X/L along the adhesive upper side
Fig. 4.44.c : ϕ vs X/L along the adhesive upper side
Fig. 4.44.d : σ_1 vs X/L along the adhesive upper side
Fig. 4.44.e : τ_{max} vs X/L along the adhesive upper side

CC) Dynamic Analysis:

. The effect of the cantilever depth inside the joint casing

Fig. 4.45.a : $\bar{f}$ vs the joint number
Fig. 4.45.b : f vs the joint number
Fig. 4.46.a : $T1$ vs X/L along the beam axis
Fig. 4.46.b : $T2$ vs X/L along the beam axis
Fig. 4.46.c : σ_1 vs X/L along the adhesive upper side
Fig. 4.46.d : ϕ vs X/L along the adhesive upper side
Fig. 4.46.e : τ_{max} vs X/L along the adhesive upper side

. The effect of the joint casing tapering

Fig. 4.47.a : $\bar{f}$ vs the joint number
Fig. 4.47.b : f vs the joint number
Fig. 4.48.a : $T1$ vs X/L along the beam axis
Fig. 4.48.b : $T2$ vs X/L along the beam axis
Fig. 4.48.c : σ_1 vs X/L along the adhesive upper side
Fig. 4.48.d : ϕ vs X/L along the adhesive upper side
Fig. 4.48.e : τ_{max} vs X/L along the adhesive upper side

. The effect of the surface waviness

Fig. 4.49.a : δ vs the joint number
Fig. 4.49.b : δ vs the joint number
Fig. 4.50.a : τ_1 vs X/L along the beam axis
Fig. 4.50.b : τ_2 vs X/L along the beam axis
Fig. 4.50.c : σ_1 vs X/L along the adhesive upper side
Fig. 4.50.d : ϕ vs X/L along the adhesive upper side
Fig. 4.50.e : τ_{max} vs X/L along the adhesive upper side

. The adhesive fillet effect

Fig. 4.51.a : δ vs the joint number
Fig. 4.51.b : δ vs the joint number
Fig. 4.52.a : τ_1 vs X/L along the beam axis
Fig. 4.52.b : τ_2 vs X/L along the beam axis
Fig. 4.52.c : σ_1 vs X/L along the adhesive upper side
Fig. 4.52.d : ϕ vs X/L along the adhesive upper side
Fig. 4.52.e : τ_{max} vs X/L along the adhesive upper side

. The joint casing clamping effect

Fig. 4.53.a : δ vs the joint number
Fig. 4.53.b : δ vs the joint number
Fig. 4.54.a : δ vs the joint number
Fig. 4.54.b : δ vs the joint number
Fig. 4.55.a : δ vs the joint number
Fig. 4.55.b : δ vs the joint number
Fig. 4.56.a : τ_1 vs X/L along the beam axis
Fig. 4.56.b : τ_2 vs X/L along the beam axis
Fig. 4.56.c : σ_1 vs X/L along the adhesive upper side
Fig. 4.56.d : ϕ vs X/L along the adhesive upper side
Fig. 4.56.e : τ_{max} vs X/L along the adhesive upper side

: Bonding of dissimilar adherends

Fig. 4.57.a : δ vs the joint number
Fig. 4.57.b : δ vs the joint number
Fig. 4.58.a : δ vs the joint number
Fig. 4.58.b : δ vs the joint number
Fig. 4.59.a : δ vs the joint number
Fig. 4.59.b : δ vs the joint number
Fig. 4.60.a : δ vs the joint number
Fig. 4.60.b : δ vs the joint number
Fig. 4.61.a : δ vs the joint number
Fig. 4.61.b : δ vs the joint number
Fig. 4.62.a : δ vs the joint number
Fig. 4.62.b : δ vs the joint number
Fig. 4.63.a : δ vs the joint number
Fig. 4.63.b : δ vs the joint number
Fig. 4.64.a : δ vs the joint number
Fig. 4.64.b : δ vs the joint number
Fig. 4.65.a : τ_1 vs X/L along the beam axis

Fig. 4.65.b : T_2 vs X/L along the beam axis
Fig. 4.65.c : σ_1 vs X/L along the adhesive upper side
Fig. 4.65.d : ϕ vs X/L along the adhesive upper side
Fig. 4.65.e : τ_{max} vs X/L along the adhesive upper side

Chapter One

Background and Introductory Material

Chapter One

1.1) Historical Review

Adhesively bonded joints have been analysed by various people over the last fifty years using closed form techniques of various complexity, besides other numerical methods such as the finite difference method.

The earliest analyses of adhesive bonded joints were purely elastic and were analysed with the aid of the closed form approach. The first analysis is that of Volkersen who in 1938 [1], computed adhesive shear stress distribution along the lap length caused by the differential straining of adherends in which he assumed the lengthwise stretching of the adhesive to remain straight. This cause the stress concentrations at the ends of the overlap. Volkersen did not examine the tearing stress resulting from bending of the members due to ecentricity of the load path.

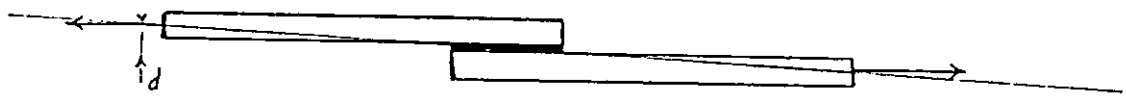

-----> (Bending Moment = Fd, due eccentricity in load path by a distance d)

Fig 1.1 : The Eccentricity of the Load Path in a Lap Joint

While Golland and Reissner in 1944 [2], presented the equivalent analysis for an asymmetrical single lap joint such that the normal stresses in the adhesive layer cause transverse deflection; besides the shear and tear stresses; and the adherend bending causes the overlap region to rotate due to the eccentricity in the load path by a distance (d). This case is considered as a large displacement problem. This analysis was simplified as being in-plane strain.

An attempt to combine the Golland and Reissner theory with Volkersen's theory was done by Plantema [3] in order to compute the differential strain of the members and the stress distribution at the end of the lap joint overlap.

Cornell [4] determined the stress distribution along the lap joint on the assumption that the adherends behave like simple beams and the lower modulus adhesive layer can be represented by a number of shear and tension springs. This conclusion meets with my results, since the variation of the stresses along the adhesive upper and lower sides of the double containment joint, as will be explained later, (fig. 4.*.1) behaves approximately linearly, besides that the beam of this joint behaves as the cantilever since it is bonded to containment from one side.

Reissner and Lubkin [5] considered the distribution of stress in the adhesive lap joint between thin cylindrical tubes of circular cross-section loaded in tension. Lubkin has established conditions under which a flat or tubular joint can have uniformly dis-

tributed stresses in the adhesive and has given a formula for these stresses for the case in which the adhesive obeys the linear stress-strain relation.

Renton and Vinson [6], Sirinivas [7] and Allman [8] in whose investigations differential equations are set up for the closed form solution in order to consider the effect of bending, transverse normal and shear deformations, were assuming a squared edged adhesive layer at the end of the lap joint overlap, while Mylonas [9] found that the change of inclination of the adhesive free surface to the adherend moves out the stress concentration to near the trailing corner somewhere of contact angle of 50 degree and 40 degrees. When an adhesive fillet was included the highest stress was found at 45 degrees to the surface of the adherend and near the adherend corner. Mylonas, also investigated experimentally various edge shapes of the lap joint with the aid of photoelastic techniques.

Maclaren [10], August 1957, examined the effect of deformation in a bonded lap joint due to applied load; Golland and Reissner [11]; used photo-elasticity to cover a wider range of such deformations. Hahn [12] showed that the adhesive shear stresses were highest at the corners of the lap joint. This observation agrees with the stress distribution of the present work where σ_x, σ_y , τ_{xy}, σ_T and τ_{max} increase along the adhesive upper and lower sides for the beam inner left corner towards the adhesive free edge.

In the classical analyses of Volkersen [1] and of Golland and Reissner[11] it was assumed that the adhesive shear stresses could be represented as constant across the adhesive thickness. In fact, this is not the case because of the stress-free state of the exposed end of the adhesive layer. The consequence of this increase of the analysis has been to reduce the predicted peak elastic shear substantially and to move it inboard, away from the very end of overlap. Allman [8] has allowed for a linear variation of the peel stress across the adhesive thickness, although his adhesive shear stress is constant. Approximately it is accepted as will be shown in the present work to consider the stress variation across the adhesive thickness as constant, but for low scale of bond thickness, specifically at the free end.

In 1980, Hart Smith [13] worked out several bonded joint configurations such as the uniform or stepped and tapered adherends, using the closed form solution. He concluded that for the long overlap structural joints the strength is independent of overlap. Therefore for a short overlap the strength is sensitive up to a certain limit in which it afterwards becomes independent. In the present work, it is concluded that for a double containment joint, the stresses in the adhesive sides are sensitive up to 75% of the beam depth afterwhich the stresses are insensitive, as shown in fig 4.*.1. Hart Smith has accounted for the adherend bending for both the single and double lap joints as boundary conditions at the ends of the overlap for determining the peaks of the adhesive shear and peel stresses, but the solution is approximated, since Smith has neglected the out of plane bending which induces the peel stresses.

Lubkin [5], Wah [14] and Webber [15] analysed the scarf joints while Thamm [16] studied the scarf and bevel joints. The latter concluded tapering to be of little significance unless a fine edge could be obtained which is difficult to be maintained. This observation meets with mine since it is found that the stress distribution along the adhesive sides isn't appreciably sensitive to the casing tapering of the double containment joint except for the scarfed one which is not practical.

دار المنظومة
DAR ALMANDUMAH
الرواد في قواعد المعلومات العربية

العنوان:	The Investigation of the effect of Various Parameters of Double Containment Joint of a Composite Structure
المؤلف الرئيسي:	Krayyem, Ahmad Mohammed
مؤلفين آخرين:	Sadek, Medhat M.(Super)
التاريخ الميلادي:	1990
موقع:	الكويت
الصفحات:	1 - 466
رقم MD:	586776
نوع المحتوى:	رسائل جامعية
اللغة:	English
الدرجة العلمية:	رسالة ماجستير
الجامعة:	جامعة الكويت
الكلية:	كلية الهندسة
الدولة:	الكويت
قواعد المعلومات:	Dissertations
مواضيع:	الهندسة الميكانيكية، تكنولوجيا التثبيت
رابط:	https://search.mandumah.com/Record/586776

© 2020 دار المنظومة. جميع الحقوق محفوظة.
هذه المادة متاحة بناء على الإتفاق الموقع مع أصحاب حقوق النشر، علما أن جميع حقوق النشر محفوظة. يمكنك تحميل أو طباعة هذه المادة للاستخدام الشخصي فقط، ويمنع النسخ أو التحويل أو النشر عبر أي وسيلة (مثل مواقع الانترنت أو البريد الالكتروني) دون تصريح خطي من أصحاب حقوق النشر أو دار المنظومة.

المنارة للاستشارات
www.manaraa.com

The Investigation of the effect of Various Parameters of Double Containment Joint of a Composite Structure

Prepared by

Ahmad Mohammed Krayyem

Supervised by

Prof. Medhat M Sadek

A Thesis submitted for the Partial fulfillment for the Degree of Master of Science at the University of Kuwait

To my parents and brother Emad for their encouragement and help.

جامعة الكويت

البحث في تاثير العوامل المختلفة علي الربطة مزدوجة الاحتواء والمؤلفة من عدة أجزاء

أطروحة في الهندسة الميكانيكية

إعداد
م. أحمد محمد كريم

إشراف
أ.د. مدحت صادق

سلم كتحقيق جزئي لمتطلبات درجة ماجستير
علوم في الهندسة الميكانيكية
أبريل (نيسان) ١٩٩٠ م

حقوق النشر ١٩٩٠م ل : أحمد محمد كريم